frontiers
in Oncology

Potential clinical roles for metabolic imaging with hyperpolarized [1-13C]pyruvate

Kevin Brindle[1*], Eva Serrao[1]

[1]Cancer Research UK Cambridge Institute, University of Cambridge, United Kingdom

This Provisional PDF corresponds to the article as it appeared upon acceptance, after peer-review. Fully formatted PDF and full text (HTML) versions will be made available soon.

Conflict of interest statement

The authors declare a potential conflict of interest and state it below.

KMB's lab has a reseach agreement with GE Healthcare (GEH) and holds patents on DNP technology with GEH.

Potential clinical roles for metabolic imaging with hyperpolarized [1-^{13}C]pyruvate

Eva M. Serrao[1, 2] and Kevin M. Brindle[1,2]†

[1]Cancer Research UK Cambridge Institute, University of Cambridge, Li Ka Shing Centre, Robinson Way, Cambridge CB2 0RE, UK.

[2]Department of Biochemistry, University of Cambridge, Tennis Court Road, Cambridge CB2 1GA, UK

Abbreviations: ^{18}FDG, ^{18}Fluorodeoxyglucose; PET, positron emission tomography; MRS, magnetic resonance spectroscopy; MRSI, magnetic resonance spectroscopic imaging.

†Corresponding author: Prof. Kevin M. Brindle, Cancer Research UK Cambridge Institute, Li Ka Shing Centre, Robinson Way, Cambridge CB2 0RE, UK.

Tel. +44 1223 769647; Fax. +44 1223 769510

Email: kmb1001@cam.ac.uk

Keywords: cancer, metabolism, imaging, hyperpolarized, pyruvate, therapy monitoring.

Clinical oncology relies increasingly on biomedical imaging, with anatomical imaging, especially using CT and ^{1}H-MRI, forming the mainstay of patient assessment, from diagnosis to treatment monitoring. However, the need for further improvements in specificity and sensitivity, coupled with imaging techniques that are reaching their limit of clinically attainable spatial resolution, has resulted in the emergence and growing use of imaging techniques with additional functional read-outs, such as ^{18}FDG-PET and multi-parametric MRI. These techniques add a new dimension to our understanding of the biological behavior of tumors, allowing a more personalized approach to patient management.

An important functional imaging target in cancer is metabolism. PET measurements of ^{18}Fluorodeoxyglucose uptake, a ^{18}F labeled glucose analog, (^{18}FDG-PET), and ^{1}H-MRS measurements, have both been used to investigate tumor metabolism for diagnostic purposes. However, clinical applications of MRS have been hampered by low sensitivity and consequently low spatial and temporal resolution (Glunde and Bhujwalla, 2011). Nuclear spin hyperpolarization of ^{13}C-labelled substrates, using dynamic nuclear polarization (DNP), which radically increases the sensitivity of these substrates to detection by ^{13}C MRS (Ardenkjaer-Larsen et al., 2003), has created a renewed interest in MRS measurements of tissue metabolism. Successful translation of this technique to the clinic was achieved recently with measurements of [1-^{13}C]pyruvate metabolism in prostate cancer (Nelson et al., 2013) (see Figure 1). We explore here the potential clinical roles for metabolic imaging with hyperpolarized [1-^{13}C]pyruvate.

Dynamic nuclear polarization

DNP, which can increase the signal-to-noise ratio in the solution-state ^{13}C MR experiment by 10^4 - 10^5 fold (Brindle et al., 2011) has enabled *in vivo* imaging of various metabolites and

their enzymatic conversion into other species, as well as metabolic fluxes in central metabolic pathways, such as glycolysis (Meier et al., 2011;Harris et al., 2013;Rodrigues et al., 2014) and the tricarboxylic acid cycle (Schroeder et al., 2009;Merritt et al., 2011;Chen et al., 2012). The principle limitation of the technique is the short half-life of the polarization; for [1-^{13}C]pyruvate *in vivo* this is typically between $30 - 40$ s, which means that the hyperpolarized signal will last for $2 - 3$ minutes. Therefore the substrate, whose metabolism is to be imaged, must be transferred promptly from the polarizer, injected intravenously and then transit quickly via the circulation to the tissue of interest, where it should be taken up and metabolized rapidly (Gallagher et al., 2011;Brindle, 2015). To date numerous molecules, in addition to ^{13}C-labelled pyruvate, have been successfully hyperpolarized and their metabolism imaged, including [1,4-^{13}C$_2$]fumarate, as a marker of cell necrosis (Gallagher et al., 2009;Clatworthy et al., 2012); [U-^{2}H, U-^{13}C]glucose for assessment of glycolytic and pentose phosphate pathway activities and for detecting early treatment response (Rodrigues et al., 2014); ^{13}C-labelled bicarbonate for *in vivo* mapping of pH (Gallagher et al., 2008a); and ^{13}C-labelled urea as a marker of perfusion (Wilson et al., 2010), amongst others (Day et al., 2007;Gallagher et al., 2009;Wilson et al., 2010;Kurhanewicz et al., 2011). Despite initial interest in vascular imaging (Golman et al., 2002;Svensson et al., 2003;Mansson et al., 2006), the main focus has been on imaging metabolism in tumors (Chen et al., 2007;Day et al., 2007;Gallagher et al., 2009) and cardiac tissue (Merritt et al., 2007;Golman et al., 2008;Merritt et al., 2008;Schroeder et al., 2008;Dodd et al., 2014).

Pyruvate

Pyruvate is an important intermediate in many biochemical pathways (Denton and Halestrap, 1979). As an end product of glycolysis, pyruvate can be reduced by NADH to generate lactate, in the readily reversible reaction catalyzed by lactate dehydrogenase, or

transaminated by glutamate, in the reversible reaction catalyzed by alanine aminotransferase (ALT), to form alanine. In tissues with high levels of mitochondrial activity, such as heart muscle, pyruvate may be irreversibly decarboxylated to form carbon dioxide in the reaction catalyzed by the mitochondrial pyruvate dehydrogenase (PDH) complex (Schroeder et al., 2008). Since increased aerobic glycolysis is a well-recognized hallmark of cancer (Gatenby and Gillies, 2004;Hanahan and Weinberg, 2011) this has made it an attractive pathway to probe for diagnostic and treatment monitoring purposes (Golman et al., 2006;Day et al., 2007;Nelson et al., 2013).

Potential clinical roles

Preclinical studies have demonstrated that hyperpolarized [1-^{13}C]pyruvate is a promising probe for oncological imaging, with increased lactate labeling observed in tumors as compared to normal tissues (Golman et al., 2006;Park et al., 2010). The substrate has the potential to be used in many steps of patient management. A recent study demonstrated the potential of hyperpolarized [1-^{13}C]pyruvate as an imaging biomarker for early detection and secondary screening of pancreatic cancer, where a decrease in the hyperpolarized [1-^{13}C]alanine/[1-^{13}C]lactate ratio was observed in the progression from precursor lesions to adenocarcinoma (Serrao et al., 2015). In another study, [1-^{13}C]pyruvate detected metabolic changes prior to tumor formation (Hu et al., 2011). Additionally, in the first reported clinical trial in prostate cancer, increased lactate labeling was observed in histologically confirmed areas of disease that were not identifiable by conventional ^{1}H-MRI measurements (Nelson et al., 2013) (Figure 1). The few studies that have explored the role of [1-^{13}C]pyruvate in grading and prognosis, which were in the transgenic mouse model of prostate adenocarcinoma (TRAMP), have also produced promising results (Albers et al., 2008;Chen AP, 2008). Tumor grading by biopsy can sometimes be difficult depending on the

accessibility of the organ of interest. Translation of the DNP technique to the clinic may allow more accurate targeting of biopsy procedures. Since lactate labeling is increased in regions of hypoxia the technique also has the potential to be used for treatment planning in radiotherapy (Krishna et al., 2013;Bluff et al., 2015). Clinical assessments of tumor responses to treatment are still based largely on observed changes in tumor size (Eisenhauer et al., 2009). However, this might not always be appropriate, particularly for detection of early responses or if the drug does not result in tumor shrinkage, for example in the case of anti-angiogenic drugs (Brindle, 2008;Bohndiek et al., 2012). Additionally, treatment assessment using ^{18}FDG-PET is difficult in some organs, e.g. prostate and brain, due to both low tumor uptake and increased background uptake respectively (Brindle, 2008). Evaluation of treatment response is likely to be the clinical scenario where hyperpolarized [1-^{13}C]pyruvate will have the most impact, as it could lead to immediate changes in clinical management, allowing the clinician to change a non-responding patient to a more effective drug at an early stage (Brindle, 2008). Early assessment of treatment response could also be used to accelerate the introduction of new drugs into the clinic by providing an indication of drug efficacy in early stage clinical trials. In support of this are numerous studies showing early decreases in hyperpolarized ^{13}C label exchange between injected [1-^{13}C]pyruvate and the endogenous lactate pool in a range of cancer models following treatment with cytotoxic chemotherapy (Day et al., 2007;Witney et al., 2010), targeted drugs (Bohndiek et al., 2010;Dafni et al., 2010;Ward et al., 2010), and radiotherapy (Day et al., 2011;Bohndiek et al., 2012;Saito et al., 2015).

There is as yet no direct evidence to support the suggestion that residual disease/recurrence can be identified by increased lactate labeling. However, observations of increased lactate labeling in areas of disease and following disease progression (Nelson et al., 2013;Serrao et al., 2015) make this likely. There is, however, evidence that hyperpolarized [1-^{13}C]pyruvate

can be used to assess normal tissue toxicity, with an increase in the [1-^{13}C]lactate/[1-^{13}C]pyruvate ratio occurring in radiation-induced lung injury (Thind et al., 2013;Thind et al., 2014).

Advantages of metabolic imaging with [1-^{13}C]pyruvate

Advantages compared to [18]FDG-PET

Metabolic imaging of cancer in the clinic has principally been with [18]FDG-PET, which has been used to stage tumors and to assess treatment response. Despite its high sensitivity and capability to provide whole-body images the use of ionizing radiation is a drawback, limiting its application in children and women of reproductive age, and when multiple investigations are needed, for example as might be required for guiding treatment in an individual patient. A similar clinical role can be envisaged for [1-^{13}C]pyruvate as has been established for [18]FDG-PET. Both techniques can be used to detect increased glycolytic flux (Menzel et al., 2013) and have been shown to be comparably sensitive in detecting tumor response to treatment (Witney et al., 2009). However, since hyperpolarized [1-^{13}C]pyruvate effectively detects lactate accumulation (Gallagher et al., 2011), a defining feature of cancer metabolism, i.e. the failure to oxidize pyruvate in the presence of oxygen and reduce it instead to lactate (the "Warburg Effect"), this means that hyperpolarized [1-^{13}C]pyruvate may be more specific for detecting cancer than [18]FDG-PET. The latter detects only elevated levels of glucose uptake, which is a feature of many normal tissues as well as cancer, for example the brain. The specificity of cancer detection by hyperpolarized [1-^{13}C]pyruvate may be confounded, however, by the presence of hypoxia, which will also lead to lactate accumulation and increased lactate labeling (Bluff et al.). Another drawback of imaging with hyperpolarized [1-^{13}C]pyruvate is that the short half-life of the polarization precludes whole-body imaging.

6

Advantages compared to ^1H MRS

^{1}H-MR spectroscopy and spectroscopic imaging measurements of tissue metabolite profiles are label free and have found some applications, for example in identifying different types of brain tumor (Horska and Barker, 2010). A notable example is the detection of 2-hydroxyglutarate, which can be used to identify glioblastomas with isocitrate dehydrogenase mutations (IDH) (Choi et al., 2012). ^{1}H MRSI has also proved to be important in the prostate, where it can improve the specificity of detection and determination of tumor extent when combined with other MR imaging sequences (Johnson et al., 2014). However, detectable metabolites are present in only millimolar concentrations, as compared to tissue water protons, which are present at ~80 M, which results in long data acquisition times and limited spatial resolution. In addition data processing can be more complex and the biochemical information provided may be unfamiliar to many clinicians, which has limited routine clinical application. Moreover, ^{1}H MR spectroscopy and spectroscopic images of metabolite profiles provide a static picture of tumor metabolism. Imaging with hyperpolarized ^{13}C-labeled substrates, on the other hand, provides dynamic metabolic flux information in the form of images that can be acquired at relatively high spatial and temporal resolutions and therefore should provide an improved assessment of tumor behavior. Additionally co-injection of different hyperpolarized substrates could also provide additional functional information in the same acquisition, e.g. pyruvate for assessing glycolytic activity and urea for assessing tumor perfusion (von Morze et al., 2012).

Combining metabolic imaging with hyperpolarized [1-^{13}C]pyruvate with new technologies

PET-MRI

This is an emerging combined imaging modality with significant potential for clinical

assessment of cancer patients (Rosenkrantz et al., 2015). Simultaneous PET-MR measurements with hyperpolarized ^{13}C and ^{18}F labeled substrates would allow a multi-parametric assessment of the primary lesion and its metastases in a single imaging session, which potentially could be used to identify imaging-based phenotypes that have prognostic value and which may give a more specific readout of treatment response. For example, PET measurements of ^{18}FDG uptake assess just the first three steps in tumor glucose metabolism, that is delivery via the bloodstream, uptake on the glucose transporters and phosphorylation and trapping in the reaction catalyzed by hexokinase. ^{13}C MRSI measurements of the exchange of hyperpolarized ^{13}C label between injected [1-^{13}C]pyruvate and the endogenous lactate pool again assess delivery via the bloodstream and effectively the last two steps in the glycolytic pathway, that is the steps catalyzed by lactate dehydrogenase and the plasma membrane monocarboxylate transporters. Therefore by combining ^{18}FDG-PET and hyperpolarized [1-^{13}C]pyruvate measurements we may be able to assess flux in the entire glycolytic pathway, for example increased mitochondrial oxidation of pyruvate may have no effect on ^{18}FDG uptake but could decrease ^{13}C labeling of lactate. There are other PET probes of tumour metabolism that could also be used alongside hyperpolarized [1-^{13}C]pyruvate, and which could provide complementary information. These include ^{11}C-acetate, as a marker of fatty acid synthesis, and labelled glutamine, which can be used to assess glutaminolysis; both of which are up-regulated in tumour cells (Hensley et al., 2013) (Hosios and Vander Heiden, 2014). These PET probes may be especially useful in tumours where ^{18}FDG is ineffective, e.g. in prostate tumours (Grassi et al., 2012) and in gliomas (Venneti et al., 2015), and where the corresponding hyperpolarized ^{13}C-labelled probes are limited. For example the metabolism of hyperpolarized [1-^{13}C]acetate has been detected *in vivo* (Bastiaansen et al., 2013), however the short lifetime of the hyperpolarization means that it could not be used to monitor fatty acid synthesis, where PET studies with [1-^{11}C]acetate in

animal tumour models have shown that it can take over 60 minutes before there is substantial incorporation into the fatty acid pool (Lewis et al., 2014). In the case of [5-^{13}C]glutamine a relatively short hyperpolarization lifetime and slow metabolism (Gallagher et al., 2008b) has precluded imaging *in vivo* (Cabella et al., 2013).

Liquid biopsies

Blood and urine biomarkers, obtained from "liquid biopsies", are also evolving, providing information in a non-invasive way allied to the advantages of collection simplicity and relatively low cost. Many body fluid biomarkers have been reported for different types of cancer however few have become established in the clinic, usually because they lack specificity. A recent promising example is a panel of three urine biomarkers for early detection of pancreatic cancer (Radon et al., 2015). Rapid advances in DNA sequencing technology have allowed somatic mutations present in tumor cells to be detected and tracked in blood-borne circulating tumor DNA (ctDNA). These fragments of DNA, which have been detected with most types of cancer, have been demonstrated to have potential roles in early detection, staging, and in detecting response to therapy and acquired resistance to treatment (Murtaza et al., 2013;Bettegowda et al., 2014). Although measurements with hyperpolarized ^{13}C-labelled cell substrates and these new circulating biomarkers are still their infancy it seems likely that they will provide complementary information, for example in the assessment of tumor heterogeneity.

Conclusion and Future Directions

Imaging with hyperpolarized ^{13}C-labelled cell substrates has the potential to become a powerful tool in many steps of clinical evaluation, allowing a more personalized approach to treatment. The first clinical trial established the feasibility of imaging human tumors with

hyperpolarized [1-^{13}C]pyruvate. Since this substrate can be used to assess glycolysis, which is up regulated in many tumors, then this should make it a very general tool for oncological imaging in the clinic. Despite the biological insights that imaging with hyperpolarized ^{13}C-labelled substrates promises to deliver in the clinic, it will nevertheless have to prove itself against established and emerging clinical techniques, demonstrating that it can provide unique information that changes clinical practice.
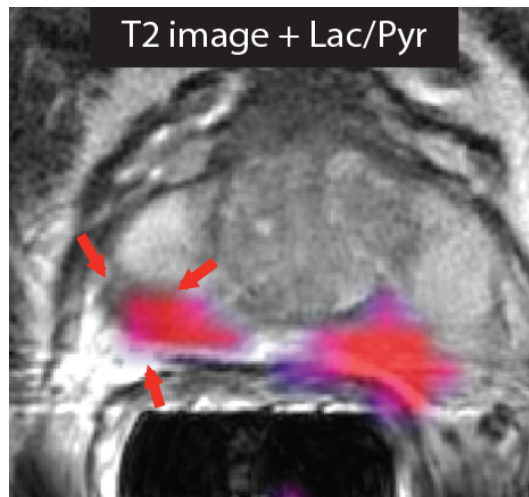
Figure 1 – Imaging prostate cancer with hyperpolarized [1-^{13}C]pyruvate. The T$_2$-weighted image of a patient with biopsy-proven bilateral prostate cancer showed only a unilateral decrease in signal intensity. However, the metabolic image ([1-^{13}C]lactate/[1-^{13}C]pyruvate ratio) detected disease on both the right and left sides of the prostate. Reproduced from (Nelson et al., 2013) with permission.

References

Albers, M.J., Bok, R., Chen, A.P., Cunningham, C.H., Zierhut, M.L., Zhang, V.Y., et al. (2008). Hyperpolarized ^{13}C lactate, pyruvate, and alanine: noninvasive biomarkers for prostate cancer detection and grading. *Cancer Res* 68**,** 8607-8615.10.1158/0008-5472.can-08-0749

Ardenkjaer-Larsen, J.H., Fridlund, B., Gram, A., Hansson, G., Hansson, L., Lerche, M.H., et al. (2003). Increase in signal-to-noise ratio of > 10,000 times in liquid-state NMR. *Proc Natl Acad Sci U S A* 100**,** 10158-10163.10.1073/pnas.1733835100

Bastiaansen, J.A., Cheng, T., Mishkovsky, M., Duarte, J.M., Comment, A., and Gruetter, R. (2013). *In vivo* enzymatic activity of acetylCoA synthetase in skeletal muscle

revealed by ^{13}C turnover from hyperpolarized [1-^{13}C]acetate to [1-^{13}C]acetylcarnitine. *Biochim Biophys Acta* 1830**,** 4171-4178.10.1016/j.bbagen.2013.03.023

Bettegowda, C., Sausen, M., Leary, R.J., Kinde, I., Wang, Y., Agrawal, N., et al. (2014). Detection of circulating tumor DNA in early- and late-stage human malignancies. *Sci Transl Med* 6**,** 224ra224.10.1126/scitranslmed.3007094

Bluff, J.E., Reynolds, S., Metcalf, S., Alizadeh, T., Kazan, S.M., Bucur, A., et al. (2015). Measurement of the acute metabolic response to hypoxia in rat tumours *in vivo* using magnetic resonance spectroscopy and hyperpolarised pyruvate. *Radiother Oncol* 116**,** 392-399.10.1016/j.radonc.2015.03.011

Bohndiek, S.E., Kettunen, M.I., Hu, D.E., and Brindle, K.M. (2012). Hyperpolarized ^{13}C spectroscopy detects early changes in tumor vasculature and metabolism after VEGF neutralization. *Cancer Res* 72**,** 854-864.10.1158/0008-5472.can-11-2795

Bohndiek, S.E., Kettunen, M.I., Hu, D.E., Witney, T.H., Kennedy, B.W., Gallagher, F.A., and Brindle, K.M. (2010). Detection of tumor response to a vascular disrupting agent by hyperpolarized ^{13}C magnetic resonance spectroscopy. *Mol Cancer Ther* 9**,** 3278-3288.10.1158/1535-7163.mct-10-0706

Brindle, K. (2008). New approaches for imaging tumour responses to treatment. *Nat Rev Cancer* 8**,** 94-107.10.1038/nrc2289

Brindle, K.M. (2015). Imaging metabolism with hyperpolarized ^{13}C-labeled cell substrates. *J Am Chem Soc* 137**,** 6418-6427.10.1021/jacs.5b03300

Brindle, K.M., Bohndiek, S.E., Gallagher, F.A., and Kettunen, M.I. (2011). Tumor imaging using hyperpolarized ^{13}C magnetic resonance spectroscopy. *Magn Reson Med* 66, 505-519.10.1002/mrm.22999

Cabella, C., Karlsson, M., Canape, C., Catanzaro, G., Colombo Serra, S., Miragoli, L., et al. (2013). *In vivo* and *in vitro* liver cancer metabolism observed with hyperpolarized [5-^{13}C]glutamine. *J Magn Reson* 232, 45-52.10.1016/j.jmr.2013.04.010

Chen, A.P., Albers, M.J., Cunningham, C.H., Kohler, S.J., Yen, Y.F., Hurd, R.E., et al. (2007). Hyperpolarized ^{13}C spectroscopic imaging of the TRAMP mouse at 3T-initial experience. *Magn Reson Med* 58, 1099-1106.10.1002/mrm.21256

Chen Ap, B.R., Zhang V, Xu D, Veeraraghavan S, Hurd Re, Nelson Sj, Kurhanewicz J, Vigneron Db (2008). Serial Hyperpolarized ^{13}C 3D-MRSI Following

Therapy in a Mouse Model of Prostate Cancer. *Proc Intl Soc Mag Reson Med*, 888

Chen, A.P., Hurd, R.E., Schroeder, M.A., Lau, A.Z., Gu, Y.P., Lam, W.W., et al. (2012). Simultaneous investigation of cardiac pyruvate dehydrogenase flux, Krebs cycle metabolism and pH, using hyperpolarized [1,2-[13]C2]pyruvate in vivo. *NMR Biomed* 25, 305-311.10.1002/nbm.1749

Choi, C., Ganji, S.K., Deberardinis, R.J., Hatanpaa, K.J., Rakheja, D., Kovacs, Z., et al. (2012). 2-hydroxyglutarate detection by magnetic resonance spectroscopy in IDH-mutated patients with gliomas. *Nat Med* 18, 624-629.10.1038/nm.2682

Clatworthy, M.R., Kettunen, M.I., Hu, D.E., Mathews, R.J., Witney, T.H., Kennedy, B.W., et

al. (2012). Magnetic resonance imaging with hyperpolarized [1,4-[13]C2]fumarate allows detection of early renal acute tubular necrosis. *Proc Natl Acad Sci U S A* 109**,** 13374-13379.10.1073/pnas.1205539109

Dafni, H., Larson, P.E., Hu, S., Yoshihara, H.A., Ward, C.S., Venkatesh, H.S., et al. (2010). Hyperpolarized ^{13}C spectroscopic imaging informs on hypoxia-inducible factor-1 and myc activity downstream of platelet-derived growth factor receptor. *Cancer Res* 70**,** 7400-7410.10.1158/0008-5472.can-10-0883

Day, S.E., Kettunen, M.I., Cherukuri, M.K., Mitchell, J.B., Lizak, M.J., Morris, H.D., et al. (2011). Detecting response of rat C6 glioma tumors to radiotherapy using hyperpolarized [1-^{13}C]pyruvate and ^{13}C magnetic resonance spectroscopic imaging. *Magn Reson Med* 65**,** 557-563.10.1002/mrm.22698

Day, S.E., Kettunen, M.I., Gallagher, F.A., Hu, D.E., Lerche, M., Wolber, J., et al. (2007). Detecting tumor response to treatment using hyperpolarized ^{13}C magnetic resonance imaging and spectroscopy. *Nat Med* 13**,** 1382-1387.nm1650 [pii] 10.1038/nm1650

Denton, R.M., and Halestrap, A.P. (1979). Regulation of pyruvate metabolism in mammalian tissues. *Essays Biochem* 15**,** 37-77

Dodd, M.S., Atherton, H.J., Carr, C.A., Stuckey, D.J., West, J.A., Griffin, J.L., et al. (2014). Impaired *in vivo* mitochondrial krebs cycle activity after myocardial infarction assessed using hyperpolarized magnetic resonance spectroscopy. *Circ Cardiovasc Imaging* 7**,** 895-904.10.1161/circimaging.114.001857

Eisenhauer, E.A., Therasse, P., Bogaerts, J., Schwartz, L.H., Sargent, D., Ford, R., et al. (2009). New response evaluation criteria in solid tumours: revised RECIST guideline (version 1.1). *Eur J Cancer* 45**,** 228-247.10.1016/j.ejca.2008.10.026

Gallagher, F.A., Bohndiek, S.E., Kettunen, M.I., Lewis, D.Y., Soloviev, D., and Brindle, K.M. (2011). Hyperpolarized ^{13}C MRI and PET: *in vivo* tumor biochemistry. *J Nucl Med* 52**,** 1333-1336.10.2967/jnumed.110.085258

Gallagher, F.A., Kettunen, M.I., Day, S.E., Hu, D.E., Ardenkjaer-Larsen, J.H., Zandt, R., et al. (2008a). Magnetic resonance imaging of pH *in vivo* using hyperpolarized ^{13}C-labelled bicarbonate. *Nature* 453**,** 940-943.10.1038/nature07017

Gallagher, F.A., Kettunen, M.I., Day, S.E., Lerche, M., and Brindle, K.M. (2008b). [13]C MR spectroscopy measurements of glutaminase activity in human hepatocellular carcinoma cells using hyperpolarized ^{13}C-labeled glutamine. *Magn Reson Med* 60**,** 253-257.10.1002/mrm.21650

Gallagher, F.A., Kettunen, M.I., Hu, D.E., Jensen, P.R., Zandt, R.I., Karlsson, M., et al. (2009). Production of hyperpolarized $[1,4-^{13}C_2]$malate from $[1,4-^{13}C_2]$fumarate is a marker of cell necrosis and treatment response in tumors. *Proc Natl Acad Sci U S A* 106**,** 19801-19806.10.1073/pnas.0911447106

Gatenby, R.A., and Gillies, R.J. (2004). Why do cancers have high aerobic glycolysis? *Nat Rev Cancer* 4**,** 891-899.10.1038/nrc1478

Glunde, K., and Bhujwalla, Z.M. (2011). Metabolic tumor imaging using magnetic resonance

spectroscopy. *Semin Oncol* 38**,** 26-41.10.1053/j.seminoncol.2010.11.001

Golman, K., Ardenkjaer-Larsen, J.H., Svensson, J., Axelsson, O., Hansson, G., Hansson, L.,

    et al. (2002). ^{13}C-angiography. *Acad Radiol* 9 Suppl 2**,** S507-510

Golman, K., Petersson, J.S., Magnusson, P., Johansson, E., Akeson, P., Chai, C.M., et al.

    (2008). Cardiac metabolism measured noninvasively by hyperpolarized ^{13}C MRI.

    Magn Reson Med 59**,** 1005-1013.10.1002/mrm.21460

Golman, K., Zandt, R.I., Lerche, M., Pehrson, R., and Ardenkjaer-Larsen, J.H. (2006).

    Metabolic imaging by hyperpolarized ^{13}C magnetic resonance imaging for *in vivo*

    tumor diagnosis. *Cancer Res* 66**,** 10855-10860.10.1158/0008-5472.can-06-2564

Grassi, I., Nanni, C., Allegri, V., Morigi, J.J., Montini, G.C., Castellucci, P., and Fanti, S.

    (2012). The clinical use of PET with ^{11}C-acetate. *Am J Nucl Med Mol Imaging* 2**,** 33-

    47

Hanahan, D., and Weinberg, R.A. (2011). Hallmarks of cancer: the next generation. *Cell* 144**,**

    646-674.10.1016/j.cell.2011.02.013

Harris, T., Degani, H., and Frydman, L. (2013). Hyperpolarized ^{13}C NMR studies of glucose

    metabolism in living breast cancer cell cultures. *NMR Biomed* 26**,** 1831-

    1843.10.1002/nbm.3024

Hensley, C.T., Wasti, A.T., and Deberardinis, R.J. (2013). Glutamine and cancer: cell

    biology, physiology, and clinical opportunities. *J Clin Invest* 123**,** 3678-

3684.10.1172/jci69600

Horska, A., and Barker, P.B. (2010). Imaging of brain tumors: MR spectroscopy and

    metabolic imaging. *Neuroimaging Clin N Am* 20**,** 293-310.10.1016/j.nic.2010.04.003

Hosios, A.M., and Vander Heiden, M.G. (2014). Acetate metabolism in cancer cells. *Cancer*

    Metab 2.10.1186/s40170-014-0027-y

Hu, S., Balakrishnan, A., Bok, R.A., Anderton, B., Larson, P.E., Nelson, S.J., et al. (2011).

    ^{13}C-pyruvate imaging reveals alterations in glycolysis that precede c-Myc-induced

    tumor formation and regression. *Cell Metab* 14**,** 131-142.10.1016/j.cmet.2011.04.012

Johnson, L.M., Turkbey, B., Figg, W.D., and Choyke, P.L. (2014). Multiparametric MRI in

    prostate cancer management. *Nat Rev Clin Oncol* 11**,** 346-

    353.10.1038/nrclinonc.2014.69

Krishna, M.C., Matsumoto, S., Saito, K., Matsuo, M., Mitchell, J.B., and Ardenkjaer-Larsen,

    J.H. (2013). Magnetic resonance imaging of tumor oxygenation and metabolic profile.

    Acta Oncol 52**,** 1248-1256.10.3109/0284186x.2013.819118

Kurhanewicz, J., Vigneron, D.B., Brindle, K., Chekmenev, E.Y., Comment, A., Cunningham,

    C.H., et al. (2011). Analysis of cancer metabolism by imaging hyperpolarized nuclei:

    prospects for translation to clinical research. *Neoplasia* 13**,** 81-97

Lewis, D.Y., Boren, J., Shaw, G.L., Bielik, R., Ramos-Montoya, A., Larkin, T.J., et al.

    (2014). Late Imaging with [1-^{11}C]Acetate Improves Detection of Tumor Fatty Acid

Synthesis with PET. *J Nucl Med* 55**,** 1144-1149.10.2967/jnumed.113.134437

Mansson, S., Johansson, E., Magnusson, P., Chai, C.M., Hansson, G., Petersson, J.S., et al. (2006). [13]C imaging-a new diagnostic platform. *Eur Radiol* 16**,** 57-67.10.1007/s00330-005-2806-x

Meier, S., Karlsson, M., Jensen, P.R., Lerche, M.H., and Duus, J.O. (2011). Metabolic pathway visualization in living yeast by DNP-NMR. *Mol Biosyst* 7**,** 2834-2836.10.1039/c1mb05202k

Menzel, M.I., Farrell, E.V., Janich, M.A., Khegai, O., Wiesinger, F., Nekolla, S., et al. (2013). Multimodal assessment of *in vivo* metabolism with hyperpolarized [1-^{13}C]MR spectroscopy and ^{18}F-FDG PET imaging in hepatocellular carcinoma tumor-bearing rats. *J Nucl Med* 54**,** 1113-1119.10.2967/jnumed.112.110825

Merritt, M.E., Harrison, C., Sherry, A.D., Malloy, C.R., and Burgess, S.C. (2011). Flux through hepatic pyruvate carboxylase and phosphoenolpyruvate carboxykinase detected by hyperpolarized ^{13}C magnetic resonance. *Proc Natl Acad Sci U S A* 108**,** 19084-19089.10.1073/pnas.1111247108

Merritt, M.E., Harrison, C., Storey, C., Jeffrey, F.M., Sherry, A.D., and Malloy, C.R. (2007). Hyperpolarized ^{13}C allows a direct measure of flux through a single enzyme-catalyzed step by NMR. *Proc Natl Acad Sci U S A* 104**,** 19773-19777.10.1073/pnas.0706235104

Merritt, M.E., Harrison, C., Storey, C., Sherry, A.D., and Malloy, C.R. (2008). Inhibition of

carbohydrate oxidation during the first minute of reperfusion after brief ischemia: NMR detection of hyperpolarized $^{13}CO_2$ and $H^{13}CO_3$. *Magn Reson Med* 60**,** 1029-1036.10.1002/mrm.21760

Murtaza, M., Dawson, S.J., Tsui, D.W., Gale, D., Forshew, T., Piskorz, A.M., et al. (2013). Non-invasive analysis of acquired resistance to cancer therapy by sequencing of plasma DNA. *Nature* 497**,** 108-112.10.1038/nature12065

Nelson, S.J., Kurhanewicz, J., Vigneron, D.B., Larson, P.E., Harzstark, A.L., Ferrone, M., et al. (2013). Metabolic imaging of patients with prostate cancer using hyperpolarized [1-^{13}C]pyruvate. *Sci Transl Med* 5**,** 198ra108.10.1126/scitranslmed.3006070

Park, I., Larson, P.E., Zierhut, M.L., Hu, S., Bok, R., Ozawa, T., et al. (2010). Hyperpolarized ^{13}C magnetic resonance metabolic imaging: application to brain tumors. *Neuro Oncol* 12**,** 133-144.10.1093/neuonc/nop043

Radon, T.P., Massat, N.J., Jones, R., Alrawashdeh, W., Dumartin, L., Ennis, D., et al. (2015). Identification of a Three-Biomarker Panel in Urine for Early Detection of Pancreatic Adenocarcinoma. *Clin Cancer Res* 21**,** 3512-3521.10.1158/1078-0432.ccr-14-2467

Rodrigues, T.B., Serrao, E.M., Kennedy, B.W., Hu, D.E., Kettunen, M.I., and Brindle, K.M. (2014). Magnetic resonance imaging of tumor glycolysis using hyperpolarized ^{13}C-labeled glucose. *Nat Med* 20**,** 93-97.10.1038/nm.3416

Rosenkrantz, A.B., Friedman, K., Chandarana, H., Melsaether, A., Moy, L., Ding, Y.S., et al. (2015). Current Status of Hybrid PET/MRI in Oncologic Imaging. *AJR Am J*

Roentgenol, 1-11.10.2214/ajr.15.14968

Saito, K., Matsumoto, S., Takakusagi, Y., Matsuo, M., Morris, H.D., Lizak, M.J., et al.
(2015). 13C-MR spectroscopic imaging with hyperpolarized [1-^{13}C]pyruvate detects
early response to radiotherapy in SCC tumors and HT-29 tumors. *Clin Cancer
Res*.10.1158/1078-0432.ccr-14-1717

Schroeder, M.A., Atherton, H.J., Ball, D.R., Cole, M.A., Heather, L.C., Griffin, J.L., et al.
(2009). Real-time assessment of Krebs cycle metabolism using hyperpolarized [13]C
magnetic resonance spectroscopy. *FASEB J* 23**,** 2529-2538.10.1096/fj.09-129171

Schroeder, M.A., Cochlin, L.E., Heather, L.C., Clarke, K., Radda, G.K., and Tyler, D.J.
(2008). *In vivo* assessment of pyruvate dehydrogenase flux in the heart using
hyperpolarized carbon-13 magnetic resonance. *Proc Natl Acad Sci U S A* 105**,** 12051-
12056.10.1073/pnas.0805953105

Serrao, E.M., Kettunen, M.I., Rodrigues, T.B., Dzien, P., Wright, A.J., Gopinathan, A., et al.
(2015). MRI with hyperpolarised [1-^{13}C]pyruvate detects advanced pancreatic
preneoplasia prior to invasive disease in a mouse model. *Gut*.10.1136/gutjnl-2015-
310114

Svensson, J., Mansson, S., Johansson, E., Petersson, J.S., and Olsson, L.E. (2003).
Hyperpolarized ^{13}C MR angiography using trueFISP. *Magn Reson Med* 50**,** 256-
262.10.1002/mrm.10530

Thind, K., Chen, A., Friesen-Waldner, L., Ouriadov, A., Scholl, T.J., Fox, M., et al. (2013).

Detection of radiation-induced lung injury using hyperpolarized ^{13}C magnetic resonance spectroscopy and imaging. *Magn Reson Med* 70**,** 601-609.10.1002/mrm.24525

Thind, K., Jensen, M.D., Hegarty, E., Chen, A.P., Lim, H., Martinez-Santiesteban, F., et al. (2014). Mapping metabolic changes associated with early Radiation Induced Lung Injury post conformal radiotherapy using hyperpolarized ^{13}C-pyruvate Magnetic Resonance Spectroscopic Imaging. *Radiother Oncol* 110**,** 317-322.10.1016/j.radonc.2013.11.016

Venneti, S., Dunphy, M.P., Zhang, H., Pitter, K.L., Zanzonico, P., Campos, C., et al. (2015). Glutamine-based PET imaging facilitates enhanced metabolic evaluation of gliomas in vivo. *Sci Transl Med* 7**,** 274ra217.10.1126/scitranslmed.aaa1009

Von Morze, C., Larson, P.E., Hu, S., Yoshihara, H.A., Bok, R.A., Goga, A., et al. (2012). Investigating tumor perfusion and metabolism using multiple hyperpolarized ^{13}C compounds: HP001, pyruvate and urea. *Magn Reson Imaging* 30**,** 305-311.10.1016/j.mri.2011.09.026

Ward, C.S., Venkatesh, H.S., Chaumeil, M.M., Brandes, A.H., Vancriekinge, M., Dafni, H., et al. (2010). Noninvasive detection of target modulation following phosphatidylinositol 3-kinase inhibition using hyperpolarized ^{13}C magnetic resonance spectroscopy. *Cancer Res* 70**,** 1296-1305.10.1158/0008-5472.can-09-2251

Wilson, D.M., Keshari, K.R., Larson, P.E., Chen, A.P., Hu, S., Van Criekinge, M., et al. (2010). Multi-compound polarization by DNP allows simultaneous assessment of

multiple enzymatic activities *in vivo*. *J Magn Reson* 205**,** 141-147.10.1016/j.jmr.2010.04.012

Witney, T.H., Kettunen, M.I., Day, S.E., Hu, D., Neves, A.A., Gallagher, F.A., et al. (2009). A Comparison between Radiolabeled Fluorodeoxyglucose Uptake and Hyperpolarized ^{13}C-Labeled Pyruvate Utilization as Methods for Detecting Tumor Response to Treatment12. *Neoplasia* 11**,** 574-582

Witney, T.H., Kettunen, M.I., Hu, D.E., Gallagher, F.A., Bohndiek, S.E., Napolitano, R., and Brindle, K.M. (2010). Detecting treatment response in a model of human breast adenocarcinoma using hyperpolarised [1-^{13}C]pyruvate and [1,4-[13]C$_2$]fumarate. *Br J Cancer* 103**,** 1400-1406.10.1038/sj.bjc.6605945

Figure 1.TIFF